Journal of Naval Architecture and Marine Engineering
December, 2023
http://dx.doi.org/10.3329/jname.v20i2.61193 *http://www.banglajol.info*

VISCO-ELASTIC IMPACTS ON AN UNSTEADY MHD FLOW PAST A CONSTANT SLANTED PLATE IN THE PRESENCE OF VISCOUS DISSIPATION, RADIATION AND CHEMICALLY REACTIVE SPECIES: A NUMERICAL STUDY

A. Nayak[1,*] and C. Rath[2]

[1]Department of Mathematics, School of Applied Sciences, Kalinga Institute of Industrial Technology (KIIT) Deemed to be University, Bhubaneswar-751024, Odisha, India. E-mail: anita.nayakfma@kiit.ac.in

[2]Department of Mathematics, School of Applied Sciences, Kalinga Institute of Industrial Technology (KIIT) Deemed to be University, Bhubaneswar-751024, Odisha, India. E-mail: 2081138@kiit.ac.in

Abstract:

A numerical investigation of the natural convection magnetohydrodynamic (MHD) flow of a visco-elastic, incompressible, and electricity-conducting fluid in a medium with porosity is carried out. The novelty of the study is to examine the impact of visco-elasticity on MHD boundary layer flow, which plays a crucial role in engineering and industrial applications. The model differential equations obtained are in a coupled form which are highly non-linear. The non-dimensional partial differential equations are simplified numerically by employing Crank-Nicolson finite difference scheme. The impact of vital parameters of the flow are discussed and presented graphically. Also, the outcomes of the physical parameters, such as skin friction, heat transfer rate, and mass transfer rate, are derived and analyzed through tables. It is observed that the visco-elastic parameter enhances the velocity profiles in the whole flow region. Also, the velocity gradient growths with the higher value of the visco-elastic parameter and the enhanced value of the magnetic parameter diminishes the profile of velocity.

Keywords: Visco-elastic fluid, magnetohydrodynamic flow, chemical reaction, viscous dissipation, porous medium, Crank-Nicolson finite difference scheme.

NOMENCLATURE

B	magnetic field (Tesla)	Q	dimensionless heat absorption parameter
C'	dimensional species concentration (mol/m^3)	R_c	visco-elastic parameter
C'_w	species concentration at the plate (mol/m^3)	Sc	Schmidt number
C'_∞	ambient species concentration (mol/m^3)	Sh	Sherwood number
C	dimensionless species concentration	T'	dimensional temperature of the fluid (K)
D	mass diffusivity (m^2/s)	T'_w	temperature at the plate (K)
Ec	Eckert number	T'_∞	ambient temperature (K)
G_c	modified Grashof number	***Greek Symbols***	
G_r	thermal Grashof number	α	angle of inclination of the plate with $x' -$ axis (rad)
K'	dimensional permeability of the porous medium (m^2)	β	volumetric coefficient of thermal expansion (1/K)
K	dimensionless permeability of the porous medium	β^*	volumetric coefficient of concentration expansion (m^3/mol)
K_r	dimensional rate constant of first-order chemical reaction (1/s)	μ	dynamic viscosity (Pa s)
k_r	dimensionless rate constant of first-order chemical reaction	ν	kinematic viscosity (m^2/s)

 Received on: Aug., 2022

k_0	dimensional visco-elastic parameter (kg/m)	ρ	density of the fluid (kg/m^3)
M	Hartmann number	σ	electrical conductivity (S/m)
N	radiation parameter	τ	skin friction coefficient
Nu	Nusselt number	κ	thermal conductivity (W/mK)
Pr	Prandtl number	θ	dimensionless temperature of the fluid
Q'	dimensional heat absorption parameter (W/m^{3}K)		

1. Introduction

Numerous researchers are attracted towards studying unsteady magnetohydrodynamic (MHD) free convection flow with heat and mass transfer. Applications of MHD include MHD submarines, pharmaceutical drug manufacturing, MHD power generators and astrophysics. These and a lot more have been beautifully explained by Davidson (2016), Jayakar et al. (2018), and Sharma et al. (2019). Also, the study on MHD natural convection has attracted many authors because of its applications in aeronautics, chemical engineering, planetary magnetosphere, and electronics, and some of them are Nield and Bejan (2017), Reddy et al. (2010) and Babu and Narayana (2009).

A time-independent MHD flow inside a micro-channel concerning the effects of Hall current and an inclined magnetic field has been examined by Jha and Malgwi (2020). The Hartmann flow through a porous channel influenced by thermal radiation and buoyancy force was investigated by Verma and Makinde (2021). Das et al. (2019) studied a time-dependent magnetohydrodynamic Casson double-diffusive fluid through a permeable medium. Ali et al. (2021) scrutinized the MHD flow past a wedge influenced by Brownian diffusion and thermophoresis. Baitharu et al. (2020) have performed a numerical investigation of the MHD mixed convective flow through a non-Darcy porous medium. The radiation effect has industrial applications like furnace design, glass production, propulsion system in space technology, and plasma physics, which researchers are interested in studying. Prasad and Reddy (2008) have analyzed the mass transfer and effect of radiation parameter on a time-dependent magnetohydrodynamic laminar mixed convective flow and past on a moving plate oriented in the vertical direction and surrounded by a permeable medium. Also, the impact of radiation parameter on a magnetohydrodynamic flow past a plate oriented in the vertical direction was observed by Kumar and Varma (2011) and Endalew and Nayak (2019). Reddy et al. (2022) have utilized the Buongiorno model to analyze the convective flow of Casson nanofluid past an inclined stretching sheet. The research on the impact of radiation parameter and transfer of mass analysis on a natural convective magnetohydrodynamic flow where the medium is filled with porosity and the plate is oriented in the vertical direction with variable temperature was investigated by Pattnaik et al. (2012). Parthiban and Palani (2022) have examined micropolar fluid flowing past an exponentially stretching sheet considering heat source and chemical reaction. Magnetohydrodynamic natural convection flow past a plate oriented in the vertical direction, which is exponentially accelerated with variable temperature in the presence of radiation, has been analyzed by Rajesh and Varma (2009). Reddy et al. (2012) analyzed the heat and mass transfer characteristics of a radiative unsteady MHD fluid flowing past an inclined plate analytically. However, the study neglects the impact of viscous dissipation. Umamaheswar et al. (2013) extended the work of Reddy et al. (2012) by introducing viscous dissipation, heat source, and ohmic heating on an unsteady MHD natural convective visco-elastic fluid past a permeable plate. Sahoo et al. (2022) have recently investigated the consequences of chemical reaction and radiation on the MHD transient natural convective flow through a permeable medium. Many researchers are attentive towards studying the MHD flow of visco-elastic fluid because of its numerous applications in geophysics, geohydrology, astrophysics, chemical engineering, and biological system. Also, flow through permeable medium is helpful for the extraction of unrefined oil from the canal of rocks. Similarly, heat and mass transfer analysis has huge applications in geothermal and oil reservoirs, which researchers are interested in studying. Choudhury and Bhattacharjee (2013) investigated the MHD time-dependent natural convective viscoelastic fluid flow with mass transfer and the Dufour effect. Kar et al. (2014) have investigated the impact of viscous dissipation, radiation and heat source of Walters fluid B' past a permeable stretching sheet. Magnetohydrodynamic visco-elastic fluid flow over a stretching sheet in the vertical direction or a continuously moving plate has been observed by many investigators, such as Abel et al. (2005) and Rashidi et al. (2015). They presented excellent results under various applicable boundary conditions. Jena et al. (2018) have analyzed the transfer of mass and Soret and Dufour effects on MHD visco-elastic flow past a stretching sheet that is oriented vertically in addition to a heat sink or source. Akinbo and Olajuwon (2021) have analyzed Walters B' fluid flowing past an upright stretching sheet. Baitharu et al. (2020) have examined the flow characteristics of a

radiative second-grade fluid past a stretching sheet with heat source. Babitha et al. (2023) have addressed the MHD flow of Casson and Carreau nanofluid flowing through a permeable medium.

Recently, Barik and Dash (2014) have discussed a numerical solution to a problem on a time-dependent magnetohydrodynamic flow past an inclined heated impermeable plate where viscous dissipation and mass transfer effects are analyzed. The authors investigated the impact of the non-isothermal flow of viscous fluid along with viscous dissipation in their work. Analyzing the impact of visco-elastic fluid in industrial applications, the present work extends the problem of Barik and Dash (2014) by considering rheology in the fluid. Thereby the analysis of the transfer of mass and heat was made for a viscoelastic fluid. The governing flow system is solved numerically for the solution of equations of velocity, temperature, and mass diffusion. The impacts of the material parameters are discussed quantitatively through figures and tables. The conclusions obtained by Barik and Dash (2014) agree well with our result. The idea of the current research work is to inspect the visco-elastic impacts on an unsteady magnetohydrodynamic natural convective fluid flow past an impetuously started heated inclined impermeable plate of semi-infinite length. The study of heat and mass transfer in the existence of heat absorption, chemical reaction, and viscous dissipation was also carried out. The Crank-Nicolson finite difference method is applied to solve the problem, which is more efficient and agrees well with the work of Barik and Dash (2014) without visco-elasticity.

2. Problem Formulation

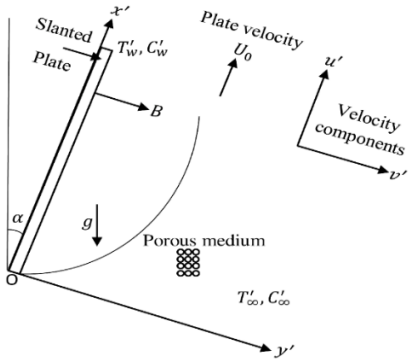

Fig. 1: The model of the problem

We have considered a natural convective two-dimensional magnetohydrodynamic unsteady flow of a viscoelastic fluid that is incompressible and electrically conducting past an impermeable plate with thermal radiation and chemical reaction. The plate is considered along the $x' -$ axis and the $y' -$ axis is normal to it. Again, due to the infinite length along the $x' -$ axis, the governing parameters taken here are not dependent on the $x' -$ spatial direction. A regular magnetic field $\vec{B} = (0, B_0)$ is applied along the $y' -$ direction perpendicular to the plate. Fig. 1 represents the model of the problem. The assumption made here is that the presence of magnetic Reynolds number and applied magnetic field is infinitesimal, for which the induced magnetic field is omitted (Cramer and Pai, 1973). The inclination of the plate is in the vertical direction with an angle α. Here, we have considered a homogeneous first-order chemical reaction occurring between the diffusive species and the fluid whose rate constant is K_r. The absence of the electric field denotes no applied voltage in the flow field. The liquid considered here has a fixed value of thermal conductivity and kinematic viscosity, and the theory due to Boussinesq has been applied to the entire flow problem. The nature of the fluid is absorbing/emitting. The nature of the radiative heat flux is described using the approximation theory due to Rosseland. In the beginning, it is taken that the surrounding fluid and the plate have the same constant concentration C'_∞ and temperature T'_∞. With increasing time, i.e., $t' > 0$, the plate has a motion with a constant velocity U_0. Also, the temperature and concentration levels are linearly increased or decreased with time. The iinstantaneous temperature and concentration of the plate are T'_w and C'_w, respectively, which are hereafter considered as constants. Considering the above assumptions, the fluid velocity, temperature, and concentration equations of the present investigation are:

$$\frac{\partial u'}{\partial t'} = g\beta(T' - T'_\infty)\cos(\alpha) + g\beta^*(C' - C'_\infty)\cos(\alpha) + \nu\frac{\partial^2 u'}{\partial y'^2} - \left(\frac{\sigma B_0^2}{\rho} + \frac{\nu}{K'}\right)u' - \frac{k_0}{\rho}\frac{\partial^3 u'}{\partial t' \partial y'^2} \tag{1}$$

$$\rho C_p \frac{\partial T'}{\partial t'} = \kappa\frac{\partial^2 T'}{\partial y'^2} - \frac{\partial q_r}{\partial y'} + \mu\left(\frac{\partial u'}{\partial y'}\right)^2 - Q'(T' - T'_\infty) \tag{2}$$

$$\frac{\partial C'}{\partial t'} = D\frac{\partial^2 C'}{\partial y'^2} - K_r(C' - C'_\infty) \tag{3}$$

The initial and boundary conditions are:

$$\begin{gathered} t' \le 0: u' = 0, T' = T'_\infty, C' = C'_\infty \; for \; all \; y' \\ t' > 0: u' = U_0, T' = T'_\infty + (T'_w - T'_\infty)At', C' = C'_\infty + (C'_w - C'_\infty)At' \; at \; y' = 0 \\ t' > 0: u' \to 0, T' \to T'_\infty, C' \to C'_\infty \; as \; y' \to \infty \end{gathered} \tag{4}$$

where $A = U_0^2/\nu$. The term q_r represents radiative heat flux, and under the theory of Rosseland approximation, it is expressed as

$$q_r = -\frac{4\sigma_1}{3\kappa_1}\frac{\partial T'^4}{\partial y'} \tag{5}$$

where σ_1 represents the constant due to Stefan-Boltzmann and κ_1 is the heat absorption coefficient. The temperature variation inside the flow is assumed to be very small, for which the linear relation between T'^4 and T'_∞ can be obtained from Taylor series expansion after ignoring higher-order terms as follows:

$$T'^4 = 4T'^3_\infty T' - 3T'^4_\infty \tag{6}$$

By using the above Eq. (5) and Eq. (6), in Eq. (2), we have,

$$\frac{\partial T'}{\partial t'} = \frac{\kappa}{\rho C_p}\frac{\partial^2 T'}{\partial y'^2} + \frac{16\sigma_1 T'^3_\infty}{3\kappa_1 \rho C_p}\frac{\partial^2 T'}{\partial y'^2} + \frac{\mu}{\rho C_p}\left(\frac{\partial u'}{\partial y'}\right)^2 - \frac{Q'}{\rho C_p}(T' - T'_\infty) \tag{7}$$

The relevant dimensionless variables of the problem are:

$$\begin{gathered} y = \frac{y'U_0}{\nu}, t = \frac{t'U_0^2}{\nu}, u = \frac{u'}{U_0}, \theta = \frac{T' - T'_\infty}{T'_w - T'_\infty}, C = \frac{C' - C'_\infty}{C'_w - C'_\infty}, Pr = \frac{\mu C_p}{\kappa}, Sc = \frac{\nu}{D}, \\ G_r = \frac{g\beta\nu(T'_w - T'_\infty)}{U_0^3}, G_c = \frac{g\beta^*\nu(C'_w - C'_\infty)}{U_0^3}, M = \frac{\sigma B_0^2 \nu}{\rho U_0^2}, Ec = \frac{U_0^2}{C_p(T'_w - T'_\infty)}, Q = \frac{Q'\nu}{\rho C_p U_0^2}, \\ K = \frac{K'U_0^2}{\nu^2}, N = \frac{\kappa\kappa_1}{4\sigma_1 T'^3_\infty}, k_r = \frac{K_r\nu}{U_0^2}, R_c = \frac{k_0 U_0^2}{\rho\nu^2} \end{gathered} \tag{8}$$

By using Eq. (8), the dimensionless form of Eqs. (1), (3), and (7) are:

$$\frac{\partial u}{\partial t} = \frac{\partial^2 u}{\partial y^2} - \left(M + \frac{1}{K}\right)u + G_r\theta\cos(\alpha) + G_c C\cos(\alpha) - R_c\frac{\partial^3 u}{\partial t \partial y^2} \tag{9}$$

$$Pr\frac{\partial \theta}{\partial t} = \left(1 + \frac{4}{3N}\right)\frac{\partial^2 \theta}{\partial y^2} + PrEc\left(\frac{\partial u}{\partial y}\right)^2 - PrQ\theta \tag{10}$$

$$\frac{\partial C}{\partial t} = \frac{1}{Sc}\frac{\partial^2 C}{\partial y^2} - k_r C \tag{11}$$

The dimensionless form of Eq. (4) is:

$$\begin{gathered} t \le 0: u = 0, \theta = 0, C = 0 \; for \; all \; y \\ t > 0: u = 1, \theta = t, C = t \; at \; y = 0 \\ t > 0: u \to 0, \theta \to 0, C \to 0 \; as \; y \to \infty \end{gathered} \tag{12}$$

After getting the distributions of the governing equations, it is also essential to observe the impacts of thermal radiation, viscous dissipation, visco-elasticity, the Nusselt number (Nu), Sherwood number (Sh) and skin friction coefficient (τ). The definition of the dimensionless form of skin friction (τ) is:

$$\tau = \frac{\tau_w}{\rho U_0^2} = \left[\frac{\partial u}{\partial y} - R_c\frac{\partial^2 u}{\partial t \partial y}\right]_{y=0} where \; \tau_w = \left[\mu\frac{\partial u'}{\partial y'} - k_0\frac{\partial^2 u'}{\partial t' \partial y'}\right]_{y'=0} \tag{13}$$

The non-dimensional local Nusselt number $Nu_{x'}$ (i.e., local surface heat flux) and local Sherwood number $Sh_{x'}$ (i.e., local surface mass flux) are:

$$Nu_{x'} = -\left[\frac{x'}{T'_w - T'_\infty}\frac{\partial T'}{\partial y'}\right]_{y'=0} then \; Nu = \frac{Nu_{x'}}{Re_{x'}} = -\left[\frac{\partial \theta}{\partial y}\right]_{y=0} \tag{14}$$

$$Sh_{x'} = -\left[\frac{x'}{C'_w - C'_\infty}\frac{\partial C'}{\partial y'}\right]_{y'=0} then \; Sh = \frac{Sh_{x'}}{Re_{x'}} = -\left[\frac{\partial C}{\partial y}\right]_{y=0} \tag{15}$$

where $Re_{x'} = \frac{U_0 x'}{\nu}$ represents the local Reynolds number.

3. Solution Procedure

The above-derived partial differential equations (9)-(11) are highly non-linear and also in coupled form. Therefore, it is impossible to find the exact solution to the above equations under boundary conditions (12). So,

the above system of equations is solved numerically by employing the Crank-Nicolson finite difference technique. The equivalent scheme for Eqs. (9)–(11) is:

$$\left(\frac{u_{i,j+1}-u_{i,j}}{\Delta t}\right)=\frac{1}{2}\left(\frac{u_{i-1,j+1}-2u_{i,j+1}+u_{i+1,j+1}}{(\Delta y)^2}+\frac{u_{i-1,j}-2u_{i,j}+u_{i+1,j}}{(\Delta y)^2}\right)$$
$$-\frac{1}{2}\left(M+\frac{1}{K}\right)\left(u_{i,j+1}+u_{i,j}\right)+\frac{1}{2}G_r\cos(\alpha)\left(\theta_{i,j+1}+\theta_{i,j}\right)+\frac{1}{2}G_c\cos(\alpha)\left(C_{i,j+1}+C_{i,j}\right)$$
$$-\frac{R_c}{2}\left(\frac{u_{i+1,j+1}-2u_{i,j+1}+u_{i-1,j+1}}{\Delta t(\Delta y)^2}-\left(\frac{u_{i+1,j}-2u_{i,j}+u_{i-1,j}}{\Delta t(\Delta y)^2}\right)\right) \quad (16)$$

$$(Pr)\left(\frac{\theta_{i,j+1}-\theta_{i,j}}{\Delta t}\right)=\frac{1}{2}\left(1+\frac{4}{3N}\right)\left(\frac{\theta_{i-1,j+1}-2\theta_{i,j+1}+\theta_{i+1,j+1}}{(\Delta y)^2}+\frac{\theta_{i-1,j}-2\theta_{i,j}+\theta_{i+1,j}}{(\Delta y)^2}\right)$$
$$-\frac{1}{2}(Q)(Pr)\left(\theta_{i,j+1}+\theta_{i,j}\right)+\frac{1}{2}(Ec)(Pr)\left(\frac{u_{i+1,j+1}-u_{i-1,j+1}}{2(\Delta y)}+\frac{u_{i+1,j}-u_{i-1,j}}{2(\Delta y)}\right)^2 \quad (17)$$

$$(Sc)\left(\frac{C_{i,j+1}-C_{i,j}}{\Delta t}\right)=\frac{1}{2}\left(\frac{C_{i-1,j+1}-2C_{i,j+1}+C_{i+1,j+1}}{(\Delta y)^2}+\frac{C_{i-1,j}-2C_{i,j}+C_{i+1,j}}{(\Delta y)^2}\right)$$
$$-\frac{1}{2}(Sc)(k_r)\left(C_{i,j+1}+C_{i,j}\right) \quad (18)$$

The notations used here are i, and j subscripts represent the network points in the $y-$ and $t-$ directions, respectively. Also, the time interval $\Delta t = t_{j+1} - t_j$ and the grid length $\Delta y = y_{i+1} - y_i$. For the discrete equations (16)–(18), the complete solutions are found using the MATLAB routine *fsolve*, which solves the non-linear system of equations. The computations done here are for air where $Pr = 0.71$,$G_r = 1.0$, $Sc = 0.22$, $G_c = 1.0$, $M = 1.0$, $N = 1.0$, $Q = 1.0$, $Ec = 0.001$, $K = 1.0$, $\alpha = \frac{\pi}{4}$, $k_r = 1.0$, $R_c = 0.05$, $\Delta y = 0.1$, and $\Delta t = 0.001$. For numerical accuracy, the results obtained here are compared with the solution obtained by Barik and Dash (2014) without viscoelasticity (i.e., $R_c = 0$). This comparison is shown in Fig. 9(b). It can be observed that the convergence between the two solutions is outstanding, which enhanced self-confidence for the numerical solution of the present study.

4. Results and Discussion

The impact of various parameters like visco-elasticity, porosity, radiation, and viscous dissipation on the flow are discussed. We have considered here $Pr = 0.71$ (air), $R_c = 0.05$ (viscoelastic fluid), $R_c = 0$ (viscous fluid), $Sc = 0.60$ (water vapor at temperature 25℃ approximately) and $Ec = 0.01$. The Eckert number represents the additional heat due to viscous dissipation, which is desirable for an incompressible fluid. The values of the different parameters like permeability (K), radiation (N), Hartmann number (M), chemical reaction (k_r), heat absorption (Q), and time (t) are considered to be positive. The cooling of the surface is due to the positive value of Ec. It is evident from Figs. 2(b), 4(a), 7(a), and 9(b) that velocity profiles decrease because of an increasing value of M, Pr, and Q, but from Figs. 2(a), 3, 5(a), 6(a), and 9(a) velocity profiles increase when the thermal Grashof number (G_r), permeability (K), Eckert number (Ec), radiation (N) and visco-elasticity (R_c) respectively increase. From Fig. 9(a), the velocity profiles increase and attain a value of approximately 4 with the increasing value of the visco-elastic parameter. The fact agrees well with the outcomes derived by Barik and Dash (2014) without viscoelasticity.

Fig. 2(a) represents the impact of G_r, the thermal Grashof number on the profiles of velocity by keeping other parameters constant. Physically, when $(G_r = 0)$ denotes the absence of free convection current, $(G_r > 0)$ denotes cooling of the plate (or heating of fluid) and $(G_r < 0)$ represents the reverse case. Therefore, the conclusion obtained here is that the rising values of (G_r) accelerate the flow field. Fig. 2(b) represents the impact of the Hartmann number (M). The profile of velocity decreases due to both visco-elasticity and viscous dissipative heat. The Lorentz force is produced by the interaction of an electrically conducting fluid with a magnetic field, and this force acts against the flow field and slows down the flow.

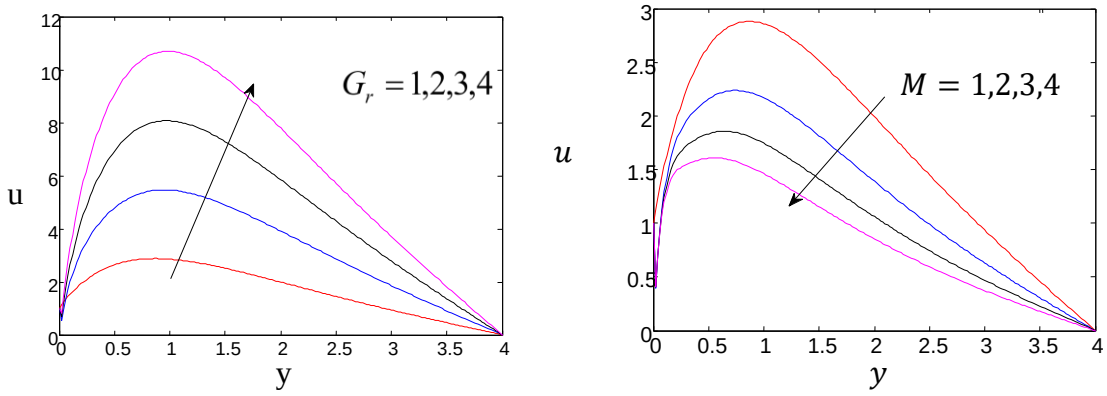

(a) (b)

Fig. 2: Profiles of velocity for a variety of values of (a) G_r and (b) M

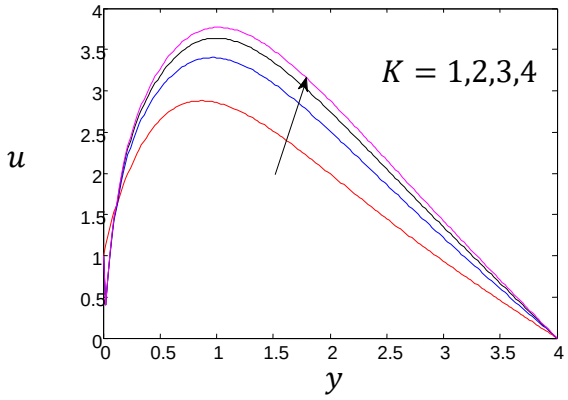

Fig. 3: Profiles of velocity for a variety of values of K

Fig. 3 illustrates the consequence of K on the profiles of velocity. The change of velocity is inconsiderable for closure and farther away from the porous plate.

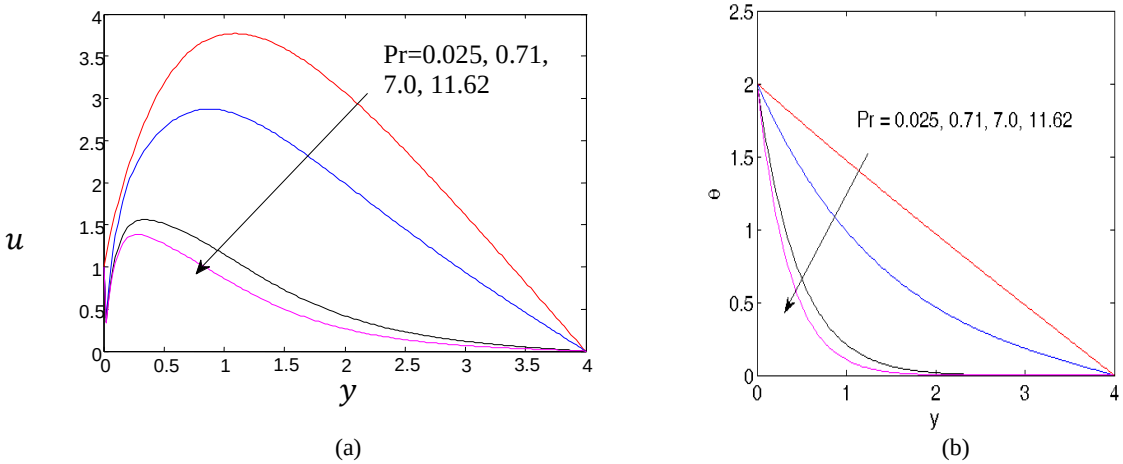

(a) (b)

Fig. 4: Profiles of (a) velocity u and (b) temperature θ for a variety of values of Pr

The effect of (Pr) on the profiles of velocity is observed in Fig. 4(a) in the existence of foreign species like in air $(Pr = 0.71)$, in mercury $(Pr = 0.025)$, in water vapor at 4℃ $(Pr = 11.62)$ and in water $(Pr = 7.00)$. The figure represents the rising value of the Prandtl number (Pr) has a reducing impact on the profiles of velocity.

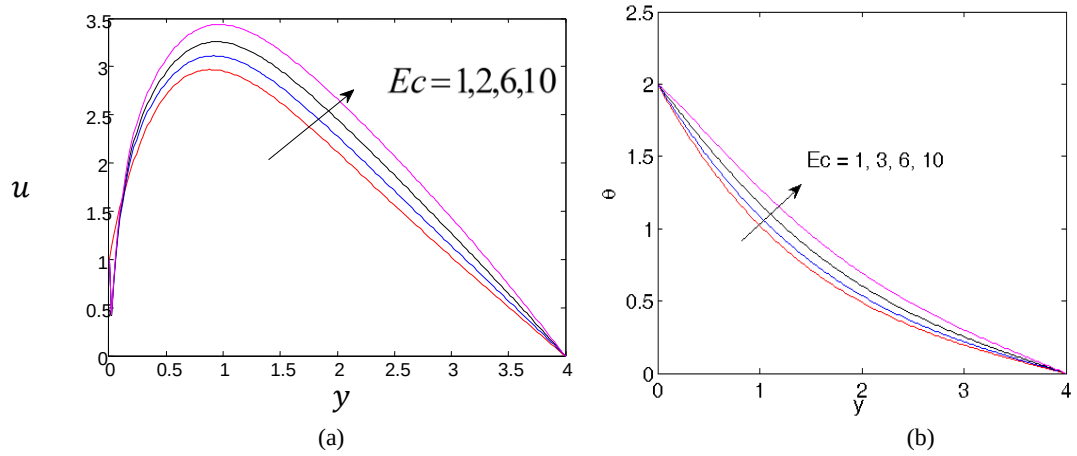

Fig. 5: Profiles of (a) velocity u and (b) temperature θ for a variety of values of Ec

Figs. 5(a) and 5(b) represent the impact of viscous dissipative heat on the profiles of velocity and temperature, respectively. Due to the rising value of viscous dissipative heat (Ec), the profiles of velocity and temperature increase with constant values of $K, N, Pr, M,$ and Q.

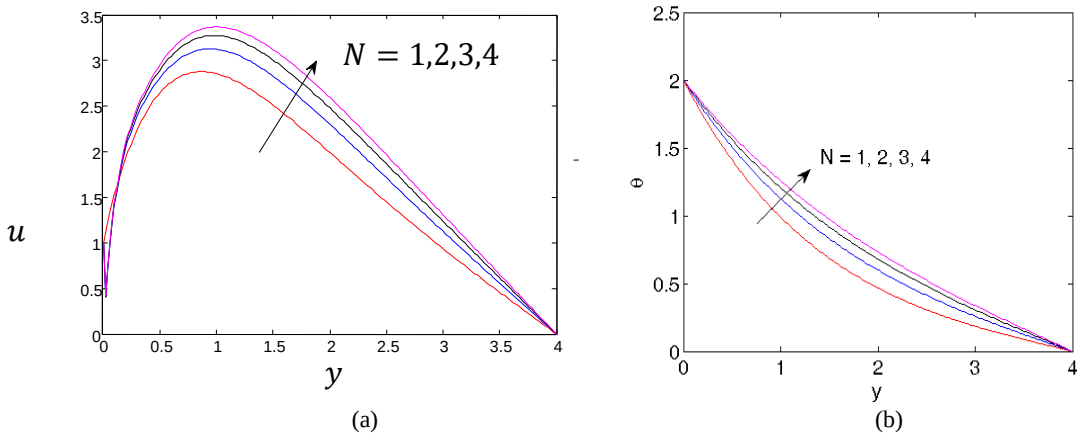

Fig. 6: Profiles of (a) velocity u and temperature θ for a variety of values of N

Figs. 6(a) and 6(b) represent the impact of N, the radiation parameter, on the profiles of velocity and temperature, respectively. The conclusion obtained here is that the rising value of N enhances both profiles. Further, Figs. 7(a) and 7(b) represent the effects of Q (the heat absorption parameter) on the profiles of velocity and temperature, respectively. Practically, the heating of fluid decreases in the occurrence of the heat absorption parameter; this is due to the weakening of the buoyancy force owing to heat absorption, which retards the rate of flow and results in a decrease in the profile of velocity and temperature. These activities are clear from the graphs.

The influence of Pr and Sc on the fields of temperature and concentration are observed from Figs. 4(b) and 8(a), respectively. Pr represents the relative significance of viscosity over thermal diffusivity, whereas Sc represents the relative significance of viscosity over mass diffusivity. It is discovered that with rising values of Pr and Sc there is a significant reduction in temperature and concentration profiles. Hence, the conclusion obtained here is that the presence of heavier species with small thermal diffusivity brings significant diminution in temperature and concentration distributions. Also, the fluid is highly conductive for a small value of Pr. Fig. 8(b) presents the result of the chemical reaction parameter k_r on the profiles of concentration. The parameter exerts a destructive influence on the concentration profile.

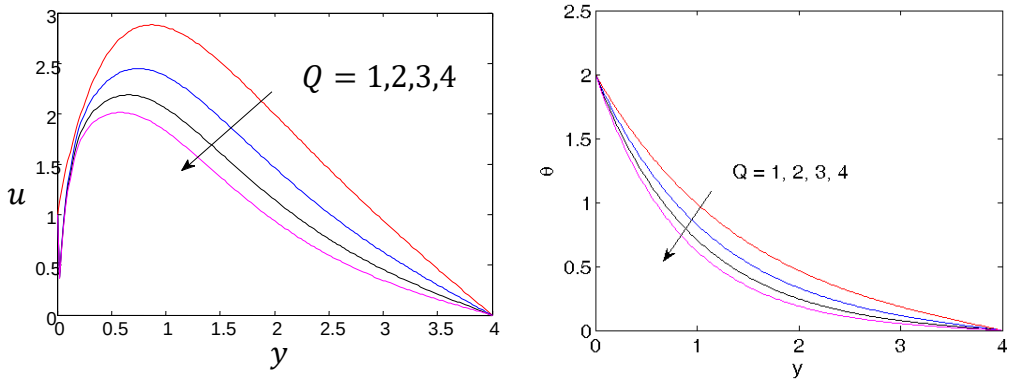

(a) (b)

Fig. 7: Profiles of (a) velocity u and (b) temperature θ for a variety of values of Q

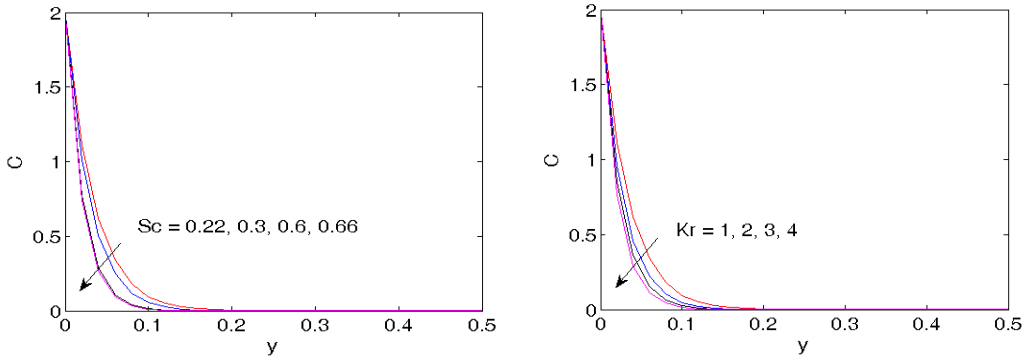

(a) (b)

Fig. 8: Profiles of concentration C for a variety of values of (a) Sc and (b) k_r

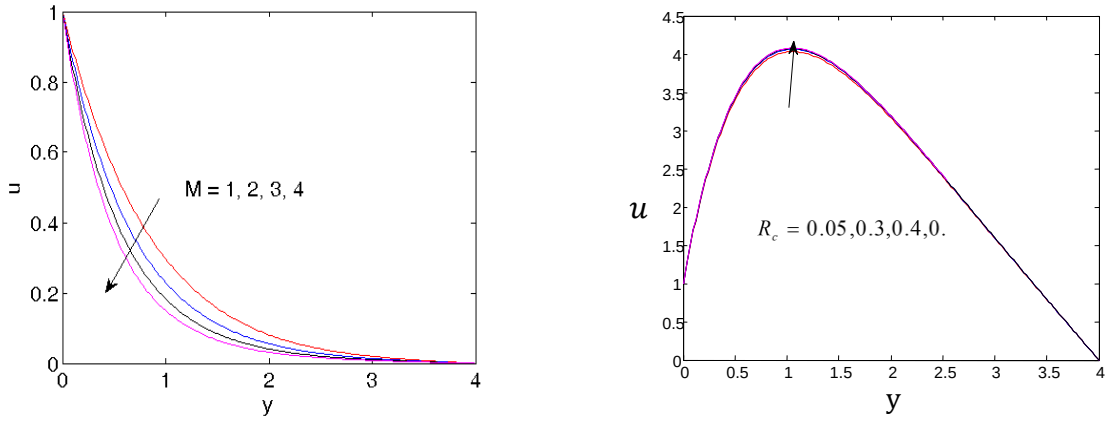

(a) (b)

Fig. 9: Profiles of velocity for a variety of values of (a) R_c and (b) M when $R_c = 0$

Fig. 9(a) explains the impact of R_c on the profiles of velocity. Plotted results conclude that there is little enhancing nature of the velocity profiles in the early stage because of the growing nature of R_c. The velocity in the horizontal direction reduces with rising values of R_c for which the boundary layer diminishes. i.e., the conclusion obtained here is that the boundary layer enlarges for larger values of R_c. The results of Fig. 9(b) conclude that the profiles of velocity have the decreasing property with the rising value of M when $R_c = 0$ and agrees well with the results obtained by Barik and Dash (2014).

The numerically calculated values of skin friction (τ) are given in Table 1. The coefficient of skin friction (τ) rises with the impact of the permeability parameter (K), thermal Grashof number (G_r), Eckert number (Ec), modified Grashof number (G_c), thermal radiation parameter (N), and visco-elastic parameter (R_c), but the opposite effect is detected with increasing values of (Pr), (M), (k_r), (Sc), and heat absorption parameter (Q). Hence, the above observation concludes that when there is a magnetic field, heavier species having high diffusivity decrease the plate shearing stress.

Table 1**:** Result of skin friction (τ).

G_r	G_c	Pr	Sc	M	K	Ec	N	R_c	Q	k_r	τ
1.0	1.0	0.71	0.22	1.0	1.0	0.001	1.0	0.05	1.0	1.0	0.1078
2.0	1.0	0.71	0.22	1.0	1.0	0.001	1.0	0.05	1.0	1.0	0.2377
3.0	1.0	0.71	0.22	1.0	1.0	0.001	1.0	0.05	1.0	1.0	0.3677
1.0	**2.0**	0.71	0.22	1.0	1.0	0.001	1.0	0.05	1.0	1.0	0.1128
1.0	**3.0**	**0.71**	0.22	1.0	1.0	0.001	1.0	0.05	1.0	1.0	0.1178
1.0	1.0	**7**	0.22	1.0	1.0	0.001	1.0	0.05	1.0	1.0	0.0566
1.0	1.0	**11.62**	0.22	1.0	1.0	0.001	1.0	0.05	1.0	1.0	0.0447
1.0	1.0	0.71	**0.30**	1.0	1.0	0.001	1.0	0.05	1.0	1.0	0.1066
1.0	1.0	0.71	**0.60**	1.0	1.0	0.001	1.0	0.05	1.0	1.0	0.1047
1.0	1.0	0.71	0.22	**2.0**	1.0	0.001	1.0	0.05	1.0	1.0	0.0839
1.0	1.0	0.71	0.22	**3.0**	1.0	0.001	1.0	0.05	1.0	1.0	0.0671
1.0	1.0	0.71	0.22	1..0	**2.0**	0.001	1.0	0.05	1.0	1.0	0.1245
1.0	1.0	0.71	0.22	1.0	**3.0**	0.001	1.0	0.05	1.0	1.0	0.1313
1.0	1.0	0.71	0.22	1.0	1.0	**0.01**	1.0	0.05	1.0	1.0	0.1078
1.0	1.0	0.71	0.22	1.0	1.0	**0.1**	1.0	0.05	1.0	1.0	0.1080
1.0	1.0	0.71	0.22	1.0	1.0	0.001	**2.0**	0.05	1.0	1.0	0.1146
1.0	1.0	0.71	0.22	1.0	1.0	0.001	**3.0**	0.05	1.0	1.0	0.1184
1.0	1.0	0.71	0.22	1.0	1.0	0.001	1.0	**0.5**	1.0	1.0	0.1132
1.0	1.0	0.71	0.22	1.0	1.0	0.001	1.0	**0.6**	1.0	1.0	2.8358
1.0	1.0	0.71	0.22	1.0	1.0	0.001	1.0	0.05	**2.0**	1.0	0.0954
1.0	1.0	0.71	0.22	1.0	1.0	0.001	1.0	0.05	**3.0**	1.0	0.0868
1.0	1.0	0.71	0.22	1.0	1.0	0.001	1.0	0.05	1.0	**2.0**	0.1056
1.0	1.0	0.71	0.22	1.0	1.0	0.001	1.0	0.05	1.0	**3.0**	0.1046

Table 2: Result of Nusselt number (Nu).

Pr	Ec	N	Q	t	Nu
0.71	1.0	1.0	1.0	1.0	0.0869
7.00	1.0	1.0	1.0	1.0	0.0286
11.62	1.0	1.0	1.0	1.0	0.0218
0.71	**2.0**	1.0	1.0	1.0	0.1231
0.71	**3.0**	1.0	1.0	1.0	0.1684
0.71	1.0	**2.0**	1.0	1.0	0.1035
0.71	1.0	**3.0**	1.0	1.0	0.1166
0.71	1.0	1.0	**2.0**	1.0	0.0628
0.71	1.0	1.0	**3.0**	1.0	0.0519
0.71	1.0	1.0	1.0	**2.0**	0.0852
0.71	1.0	1.0	1.0	**3.0**	0.0853

Table 3: Result of Sherwood number (Sh).

Sc	k_r	t	Sh
0.22	1.0	1.0	0.00259
0.30	1.0	1.0	0.00231
0.40	1.0	1.0	0.00208

0.22	**2.0**	1.0	0.00205
0.22	**3.0**	1.0	0.00189
0.22	1.0	**2.0**	0.00259
0.22	1.0	**3.0**	0.00268

The numerical value of the Nusselt number (Nu) is given in Table 2. It is observed that Nu, i.e., the heat transfer rate at the plate rises due to the thermal radiation parameter (N), Eckert number (Ec) and time (t), but it decreases in the occurrence of Q and Pr. Physically, it represents that the boundary layer heat transfer rate is favourable towards low thermal diffusivity fluid and high heat transfer dissipation.

The calculated values in Table 3 confirm that there is a reduction in the Sherwood number (Sh) with heavier species and chemical reaction parameter whereas it increases as time advances at the boundary layer. The outcomes are in great agreement with the existing results of Barik and Dash (2014).

5. Validation

The numerical outcomes of the present study are validated by comparing skin friction values with Barik and Dash (2014). The present problem was solved considering the constant parametric values: $G_c = 1.0, K = 1.0, R_c = 0, N = 1.0, Ec = 0.001, Q = 1.0, \alpha = \pi/4\,, t = 1$. Table 4 demonstrates a good agreement of our results with that of Barik and Dash (2014).

Table 4: Validation of results.

G_r	M	Pr	Sc	k_r	τ	
					Barik and Dash (2014)	Present
1.0	1.0	0.71	0.22	1.0	1.3583	1.3567
2.0	1.0	0.71	0.22	1.0	2.5584	2.5488
1.0	2.0	0.71	0.22	1.0	1.1588	1.1662
1.0	1.0	7.0	0.22	1.0	1.2124	1.2137
1.0	1.0	0.71	0.30	1.0	1.2236	1.2254
1.0	1.0	0.71	0.22	2.0	1.3115	1.3127

6. Conclusion

The governing equations of a time-dependent magnetohydrodynamic (MHD) natural convective flow past an inclined impermeable plate of a visco-elastic, electrically conducting, and incompressible fluid in a medium with permeability and radiation were framed. The term visco-elasticity is considered in the problem. The flow explained here was exposed to a transverse magnetic field. Numerical calculations and evaluations were performed using the Crank-Nicolson scheme for the coupled form of the partial, non-linear differential equations. The results were presented graphically to reveal the flow details and their properties. The following conclusions are obtained from the current problem.

- When visco-elastic parameter (R_c) was increased, the fluid velocity was increased slightly and attained a value of approximately 4.
- In the entire flow field, due to the magnetic pulling nature of the Lorentz force, the magnetic parameter (M) slows down the velocity of the fluid.
- The velocity and temperature were increased due to rising viscous dissipative heat (Ec).
- The distributions of concentration and temperature fall significantly in the existence of small thermal diffusivity and heavier species.
- Due to the enhancing value of a magnetic field, heavier species and high diffusivity decrease the shearing stress.
- The flow velocity in the entire flow domain retards with an increased value of chemical reaction parameter, Schmidt, Hartmann, Prandtl, or heat absorption parameter.

- The profile of species concentration declines with a higher value of both the Schmidt number and the chemical reaction parameter.
- There is a diminishing nature of the Sherwood number due to enhancing Schmidt number and reaction parameter values.

The immediate future work may be carried out to include the thermo-diffusion effect (Soret effect) in the concentration equation and the diffusion-thermo effect (Dufour effect) in the energy equation. This gives rise to coupled heat and mass transfer phenomena. This coupled effect finds application in isotope separation and chemical reactors. Further extension can be made considering Joulian dissipation, suction, and many more.

References

Abel, S., Prasad, K. V. and Mahaboob, A. (2005): Buoyancy force and thermal radiation effects in MHD boundary layer visco-elastic fluid flow over continuously moving stretching surface, Int. J. Therm. Sci., Vol. 44, No. 5, pp. 465–476. https://doi.org/10.1016/j.ijthermalsci.2004.08.005

Akinbo, B. J. and Olajuwon, B. I. (2021): Radiation and thermal-diffusion interaction on stagnation-point flow of Walters' B fluid toward a vertical stretching sheet, Int. Commun. Heat Mass Transf., Vol. 126, pp. 105471. https://doi.org/10.1016/j.icheatmasstransfer.2021.105471

Ali, M., Nasrin, R. and Alim, M. A. (2021): Analysis of boundaey layer nanofluid flow over a stretching permeable wedge-shaped surface with magnetic effect, J. Nav. Archit. Mar. Eng., Vol. 18, No. 1, pp. 11–24. https://doi.org/10.3329/jname.v18i1.44458

Babitha, Murthy, C. V. R. and Reddy, G. V. R. (2023): Mhd Casson and Carreau Fluid Flow Through a Porous Medium With Variable Thermal Conductivity in the Presence of Suction/Injection, J. Nav. Archit. Mar. Eng., Vol. 20, No, 1, pp. 25–35. https://doi.org/10.3329/jname.v20i1.61155

Babu, S. and Narayana, P. V. S. (2009): Effects of the Chemical Reaction and Radiation Absorption on Free Convection flow through Porous medium with Variable Suction in the presence of uniform Magnetic field, JP J. Heat Mass Transf., Vol. 3, pp. 219–234.

Baitharu, A.P., Sahoo, S. and Dash, G.C. (2020): Heat and mass transfer effect on a radiative second grade MHD flow in a porous medium over a stretching sheet, J. Nav. Archit. Mar. Eng., Vol. 17, No. 1, pp. 51–66. https://doi.org/10.3329/jname.v17i1.37777

Baitharu, A. P., Sahoo, S. N. and Dash, G. C. (2020): Numerical approach to non-Darcy mixed convective flow of non-Newtonian fluid on a vertical surface with varying surface temperature and heat source, Karbala Int. J. Mod. Sci., Vol. 6, No. 3, pp. 332–343. https://doi.org/10.33640/2405-609X.1753

Barik, R. N. and Dash, G. C. (2014): Thermal radiation effect on an unsteady magnetohydrodynamic flow past inclined porous heated plate in the presence of chemical reaction and viscous dissipation, Appl. Math. Comput., Vol. 226, pp. 423–434. https://doi.org/10.1016/j.amc.2013.09.077

Choudhury, R. and Bhattacharjee, H. K. (2013): MHD Unsteady Free Convective Visco-Elastic Fluid Flow over a Radiative Vertical Porous Plate with Dufour Effects in Presence of Chemical Reaction, Int. J. Comput. Appl., Vol. 81, pp. 19–25. https://doi.org/10.5120/13985-1995

Cramer, K. R. and Pai, S. I. (1973): Magnetofluid dynamics for engineers and applied physicists, New York: McGraw-Hill Book Company.

Das, M., Mahanta, G., Shaw, S. and Parida, S. B. (2019): Unsteady MHD chemically reactive double-diffusive Casson fluid past a flat plate in porous medium with heat and mass transfer, Heat Transf., Vol. 48, No. 5, pp. 1761–1777. https://doi.org/10.1002/htj.21456

Davidson, P. A. (2016): Introduction to Magnetohydrodynamics, Cambridge: Cambridge University Press. https://doi.org/10.1017/9781316672853

Endalew, M. F. and Nayak, A. (2019): Thermal radiation and inclined magnetic field effects on MHD flow past a linearly accelerated inclined plate in a porous medium with variable temperature, Heat Transf., Vol. 48, No. 1, pp. 42–61. https://doi.org/10.1002/htj.21367

Jayakar, R., Kumar, B. R. and Makinde, O. D. (2018): Thermo diffusion effects on MHD chemically reacting fluid flow past an inclined porous plate in a slip flow regime, Defect Diffus. Forum., Vol. 387, pp. 587–599. https://doi.org/10.4028/www.scientific.net/DDF.387.587

Jena, S., Dash, G. C. and Mishra, S. R. (2018): Chemical reaction effect on MHD viscoelastic fluid flow over a vertical stretching sheet with heat source/sink, Ain Shams Eng. J., Vol. 9, No. 4, pp. 1205–1213. https://doi.org/10.1016/j.asej.2016.06.014

Jha, B. K. and Malgwi, P. B. (2020): Effects of Hall Current and Magnetic Field Inclination on Hydromagnetic Natural Convection Flow in a Micro-Channel With Asymmetric Thermal Boundary Condition, J. Therm. Sci. Eng. Appl., Vol. 12, No. 3, pp. 031001. https://doi.org/10.1115/1.4044350

Kar, M., Sahoo, S. N., Rath, P. K. and Dash, G. C. (2014): Heat and Mass Transfer Effects on a Dissipative and Radiative Visco-Elastic MHD Flow over a Stretching Porous Sheet, Arab. J. Sci. Eng., Vol. 39, No. 5, pp. 3393–3401. https://doi.org/10.1007/s13369-014-0991-0

Kumar, A. G. V. and Varma, S. V. K. (2011): Radiation effects on MHD flow past an impulsively started exponentially accelerated vertical plate with variable temperature in the presence of heat generation, Int. J. Eng. Sci. Technol., Vol. 3, pp. 2897–2909.

Nield, D. A. and Bejan, A. (2017): Convection in Porous Media, Cham: Springer International Publishing. https://doi.org/10.1007/978-3-319-49562-0

Parthiban, R. and Palani, G. (2022): Similarity Solution of Stagnation – Spot Flow of a Micropolar Fluid Above a Flat Exponentially Elongating Penetrable Surface With Concentration and Heat Production/Absorption, J. Nav. Archit. Mar. Eng., Vol. 19, No. 1, pp. 57–70. https://doi.org/10.3329/jname.v19i1.55029

Pattnaik, J. R., Dash, G. C. and Singh, S. (2012): Radiation and Mass Transfer Effects on Mhd Free Convection Flow Through Porous Medium Past an Exponentially Accelerated Vertical Plate With Variable Temperature, Ann Fac. Eng Hunedoara- Int J Eng., Vol. 3, pp. 175–181.

Prasad, V. R. and Reddy, N. B. (2008): Radiation and mass transfer effects on an unsteady MHD convection flow past a semi-infinite vertical permeable moving plate embedded in a porous medium with viscous dissipation, Indian J. Pure Appl. Phys., Vol. 46, pp. 81–92.

Rajesh, V. and Varma, S. V. K. (2009): Radiation and mass transfer effects on MHD free convection flow past an exponentially accelerated vertical plate with variable temperature, J. Eng. Appl. Sci., Vol. 4, pp. 20–26.

Rashidi, M. M., Ali, M., Rostami, B., Rostami, P. and Xie, G. N. (2015): Heat and mass transfer for MHD viscoelastic fluid flow over a vertical stretching sheet with considering soret and dufour effects, Math. Probl. Eng., Vol. 2015, pp. 861065. https://doi.org/10.1155/2015/861065

Reddy, K. V., Vijaya, K. and Reddy, G. V. R. (2022): Buongiorno Model With Brownian and Thermophoretic Diffusion for Mhd Casson Nanofluid Over an Inclined Porous Surface, J. Nav. Archit. Mar. Eng., Vol. 19, No. 1, pp. 31–45. https://doi.org/10.3329/jname.v19i1.50863

Reddy, G. V. R., Murthy, C. V. R. and Reddy, N. B. (2010): Mass transfer and radiation effects of unsteady MHD free convective fluid flow embedded in porous medium with heat generation/absorption, J. Appl. Math. Fluid Mech., Vol. 2, pp. 85–98.

Reddy, S., Reddy, G. V. R. and Reddy, K. J. (2012): Radiation and chemical reaction effects on MHD heat and mass transfer flow inclined porous heated plate, Asian J. Curr. Eng. Math., Vol. 1, pp. 115–119.

Sahoo, S. N., Rout, P. K. and Dash, G. C. (2022): Unsteady MHD flow through porous media with temporal variation in temperature and concentration at the plate, Int. J. Ambient Energy., Vol. 43, No. 1, pp. 7977–7986. https://doi.org/10.1080/01430750.2022.2086914

Sharma, R. P., Raju, M. C., Makinde, O. D., Reddy, P. R. K. and Reddy, P. C. (2019): Buoyancy Effects on Unsteady MHD Chemically Reacting and Rotating Fluid Flow Past a Plate in a Porous Medium, Defect Diffus. Forum., Vol. 392, pp. 1–9. https://doi.org/10.4028/www.scientific.net/DDF.392.1

Umamaheswar, M., Varma, S. V. K. and Raju, M. C. (2013): Unsteady MHD Free Convective Visco-Elastic Fluid Flow Bounded by an Infinite Inclined Porous Plate in the Presence of Heat Source, Viscous Dissipation and Ohmic Heating, Int. J. Adv. Sci. Technol., Vol. 61, pp. 39–52. https://doi.org/10.14257/ijast.2013.61.05

Verma, O. P. and Makinde, O. D. (2021): Effects of Thermal Radiation and Buoyancy Force on Transient Hartmann Flow in a Channel with Permeable Walls, Lat. Am. Appl. Res., Vol. 51, No. 4, pp. 293–300. https://doi.org/10.52292/j.laar.2021.640